

## Research Article

# After Explosion-Battery Degradation Analysis using DSC and SEM

Basheer Nagoor SK<sup>1</sup>, Shanmukh Varun Teja<sup>1</sup>, Chinnadurai T<sup>1\*</sup>, Saravanan S<sup>2</sup>, Karthigai Pandiyan M<sup>3</sup>

<sup>1</sup>Department of Mechatronics, Sathyabama Institute of Science and Technology, Chennai, India

<sup>2</sup>Department of Electrical and Electronics Engineering, Sri Krishna College of Technology, Coimbatore, India

<sup>3</sup>Department of Electronics and Communication Engineering, Gitam University, Bangalore, India

E-mail: jeevadurai07@gmail.com

**Received:** 31 January 2023; **Revised:** 28 April 2023; **Accepted:** 17 May 2023

**Abstract:** Thermal management of the battery is essential for effective utilization in various environmental conditions and for long-term usage. Failure to control and monitoring of battery over-heating leads to thermal runaway, which can cause battery explosion. This paper emphasizes the overheating phenomena of lead-acid batteries in simulated heat situations. Heat is applied to the battery until it gets damaged. After the thermal damage occurred, various characterization methods were performed to analyze the thermal influence on the anode and cathode plates. The characterization methods include Differential Scanning Calorimetry (DSC) and Scanning Electron Microscopy (SEM). The DSC method is used to determine the change in glass transition temperature of anode and cathode materials, which can provide information on the material's thermal behavior at different temperatures. Likewise, SEM is used to investigate the structural morphology of anode and cathode plates. The experimental results indicate that material degradation occurs across different temperature ranges for both the anode and cathode plates. In particular, the plate's thermal influence varies at different positions, which leads to changes in plate conduction. Additionally, thermography and heat distribution images are used to identify the heat flow in the battery during the cycle period.

**Keywords:** lead-acid battery, thermography, differential scanning calorimetry, thermogravimetric analysis, scanning electron microscope

## 1. Introduction

Batteries are used to store electrical energy to provide supply for various applications.<sup>1</sup> Energy storage is essential in situations where electricity is inaccessible or when independent equipment needs to be powered without relying on the main power supply.<sup>2-3</sup> Batteries are classified into two categories such as primary and secondary batteries.<sup>4</sup> Primary batteries, such as alkaline batteries, are electrochemical cells that cannot be recharged once they are depleted and are commonly used in standalone devices. On the other hand, secondary batteries are composed of electrochemical cells that allow their chemical reactions to be reversed by applying a specific voltage in the opposite direction. Secondary batteries can be categorized based on their chemistry, including Lead-Acid batteries (LAB), Lithium-ion batteries, Nickel Cadmium batteries, and Nickel-Metal Hydride battery.<sup>5</sup> The LAB is constructed using PbO<sub>2</sub> - positive electrode,

Copyright ©2023 Chinnadurai T, et al.

DOI: <https://doi.org/10.37256/sce.4220232385>

This is an open-access article distributed under a CC BY license

(Creative Commons Attribution 4.0 International License)

<https://creativecommons.org/licenses/by/4.0/>

Pb - negative electrode and  $\text{H}_2\text{SO}_4$  - electrolyte.<sup>6</sup> In theoretical practice, the charge-discharge reversible process exchanges the material.

Additionally, the malfunction of the LAB takes place in the positive electrode as a result of degradation, corrosion of the grid, shedding, and softening, while in the negative electrode, it is due to the occurrence of hydrogen evolution and the irreversible process of sulfation.<sup>7</sup> The positive active material undergoes degradation when the grid reduces or when the coherence of  $\text{PbO}_2$  within the particles weakens. This degradation occurs as a result of repeated cycles, preventing  $\text{PbO}_2$  from effectively engaging in the charge-discharge phase.<sup>8</sup> The negative electrode becomes the limiting factor in the lifespan due to the rise in temperature and high-rate partial state of charge, resulting in shedding and softening of the positive active material and the occurrence of irreversible sulfation,<sup>9</sup> the battery can function indefinitely while operating at varying levels of charge, including participating in charge-discharge cycles with high-rate partial charging and deep cycling.<sup>8</sup>

Even though  $\text{PbSO}_4$  deposits quickly on the negative electrode surface, it is not converted into Pb and  $\text{PbO}_2$  entirely at the time of charging.<sup>10</sup> The formation of  $\text{PbSO}_4$  significantly reduces the effective surface area of the negative electrode, making the charge-discharge cycle of the electrode more complex and hindering the battery's performance. Additionally, the presence of  $\text{PbO}_2$  decreases the battery's capacity and eventually causes irreversible damage, resulting in permanent failure. Furthermore, thermal runaway, which is associated with LAB failure, leads to the evaporation of gases, thereby having detrimental effects.<sup>11</sup> Increasing acid concentration results in a greater loss of water, which alters the reversible cell voltage, necessitating a higher charge voltage based on theoretical principles. This elevated charge voltage causes the battery to become overcharged, exacerbating water loss and ultimately leading to thermal runaway of the Lead-Acid Battery (LAB).<sup>12</sup>

Temperature plays a significant role in the degradation of batteries, with Lead-Acid Batteries (LAB) being particularly susceptible to thermal issues. This is primarily due to their slower ionic diffusion and the electrochemical reactions occurring within the active materials. In addition, exposing batteries to low temperatures has two adverse effects. Firstly, it hampers the visibility of the electrochemical charge-discharge cycle, leading to a reduction in battery capacity. Secondly, it promotes the formation of a persistent layer of  $\text{PbSO}_4$  on the negative electrode, which can ultimately result in irreversible battery failure.<sup>13</sup> In general, when batteries are arranged closely together to minimize space usage, their temperature tends to rise more. This temperature increase can have adverse effects, such as heightened grid corrosion and a significant reduction in endurance. If the generated heat in the batteries is not adequately addressed, there is a risk of the temperature surpassing a specific threshold, leading to complete drying out or triggering a thermal runaway scenario.<sup>14</sup> This is also applicable to valve-regulated batteries, when the battery is in the floating state, the entire electrical energy is converted into heat as well as utilized for the recombination process.

From the above literature study, it is clearly shown that many authors discussed only thermal loading and its failure but no one concentrated on anode and cathode material thermal influence changes. Also, no one has performed the heat flux testing for the battery while high-temperature environment. To analyse of the battery anode and cathode plate behaviors in terms of temperature is performed. This study will help the researcher to understand the behaviors of batteries in high-temperature regions. In this paper, we are discussing battery failure, due to high external thermal loading. After battery failure the anode and cathode plates are removed from the casing and subjected to different testing like DSC and SEM analysis. Along with thermography is used to predict the real-time temperature variation of a battery. DSC results will help us to predict the anode and cathode plate glass transition ranges. SEM analyses are performed to identify the anode and cathode material morphology.

The following sections are as follows: 1. Experimentation, 2. Result and discussion, in this section Thermography image analysis, DSC analysis and SEM analysis are discussed.

## 2. Experimentation

The experimental setup for the proposed work is to find the thermal analysis of LAB under varying harsh environments specifically in higher temperatures. The battery used for this work kept in the chamber has a capacity of 12 V, 7 Ah with the dimensions of  $151 \times 50 \times 94$  mm, the normal operating temperature of this battery is  $25^\circ\text{C}$ , and devices purchased from commercial shops in Chennai. To mimic the higher temperature in harsh environment conditions, the

heating coils placed on both sides of the chamber which is powered by 230 V AC supply create the specific temperature. The charging and discharging process cycle is repeated in a constant time interval period at constant temperature. The discharging of the battery is done through the DC motor. The ambient temperature is measured through K-type thermocouples with an accuracy of  $\pm 2.2$  °C. This temperature is stored for further analysis purpose using NI Lab-View is installed on the desktop through and NI DAQ card. The results obtained from the thermocouple are processed with NI DAQ card. The final temperature is fed to Lab-View software to measure the continuous temperature of the chamber. The thermal imager called IR thermography is used to measure the heat flux of the battery in a real-time environment.

## 2.1 Thermography

Infrared Thermography (IRT) is a non-contact type surface utilizing a grayscale (infrared colour images) to measure temperature. The IRT image with a brighter area typically represents a high-temperature zone and a darker area indicates a lower temperature distribution.<sup>15</sup> The temperature gradients of the overall battery as well as the positive and negative terminal of the battery are measured using FLUKE Infrared Thermography (IRT) instrument - TiX-580 under temperature-varying conditions. In order to eliminate the identification of radiation emitted or reflected by the camera and operator,<sup>16</sup> the battery is kept at a 45° angle with respect to the plane of the thermal detector. To facilitate the experimental setup from the line of reflection and associated parameters, the battery is covered entirely with a black cardboard box. The camera of the thermography is fixed on a stand in such a way that it focuses exactly on the battery alone. The thermal image obtained from the IRT has two regions namely brighter and darker regions. The brighter region typically denotes a high-temperature zone whereas the darker region indicates a lower temperature distribution. Figure 1(a) shows the battery explosive starting stage, Figure 1(b) shows the battery thermal image during the explosion.

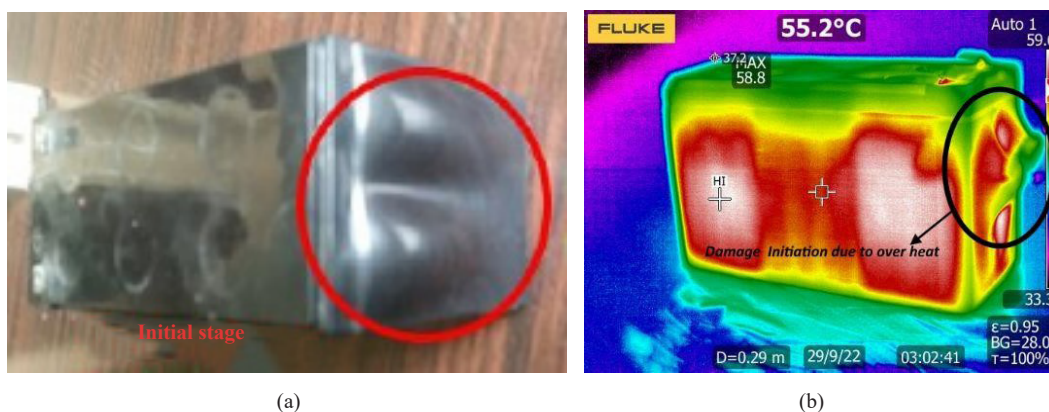


**Figure 1.** (a) Battery starts to explosive due to heating, (b) While battery explosive temperature during explosion

## 2.2 Anode and cathode plate temperature influence

The temperature influence on the battery will have a tendency to alter the anode and cathode plate structure. Structural changes happen mainly due to corrosion and internal chemical reactions. The change in structure causes the battery lead collector to change into lead dioxide or lead sulphate. These changes mainly depend on the anode and cathode plate potential, the nature of the chemical composition, the grid connection and the temperature of the cell. The corrosion on the plates was initiated because of the high internal resistance generated in the cell. Increase in internal cell temperature beyond the operating range could result in the disintegration of the anode plate. At this high temperature, repetitive charging and discharge of the battery causes expansion of the anode active mass because during the discharge cycle  $\text{PbSO}_4$  is deposited in larger volume than the positive active material  $\text{PbO}_2$ . During the charging cycle, the cell restores most of the lead dioxide but less volume when compared with the original volume of the plate. This process will result in the resistance increases in the anode plate and material disorientation. However, increases in resistance

and orientation of the material will reduce the battery lifetime and total capacity.<sup>17</sup> Figure 2(a) shows the anode plate condition after the explosion of the battery and Figure 2(b) shows the cathode plate condition after the explosion.



**Figure 2.** (a) Removed Anode plate after explosion of battery, (b) Removed cathode plate after explosion of the battery

Where 1 denotes the power terminal of the plates, 2 denotes the samples taken from near the terminal region and 3 denotes the samples taken from the bottom of the plates.

### 2.3 Differential scanning calorimetry

The study utilizes the 200F3 Maia instrument to examine samples under a temperature range of -70 to 220 degrees Celsius. The samples are then cooled from 220 to -70 degrees Celsius. The second heating phase involves raising the temperature from -70 to 220 degrees Celsius while nitrogen is present. The heating rate is set at -264 degrees Celsius per minute, and the samples are contained within an aluminum crucible with a sealed lid that has been pierced. It is anticipated that thermal degradation will occur in the presence of nitrogen, with minimal thermo-oxidation due to the small residual amount of absorbed oxygen.

### 2.4 Scanning electron microscope

To investigate the alloy changes in the battery under temperature-varying conditions due to electro-deposition and corrosion during charging as well as discharging is analyzed using Scanning Electron Microscope (SEM).<sup>18</sup> The equipment model using this analysis is Thermo-Fisher FEI Quanta 250 FEG (Field Emission Scanning Electron Microscope-FE-SEM). The sample used for SEM image is taken by removing the anode and cathode plates of the battery and washed using distilled water to naturalize the pH content. Further, these samples are dried over a day at 50 °C under vacuum conditions and then cut into triangle shapes with 2 mm thickness.

## 3. Result and discussion

The wrong usage of LAB leads to significant cause to grid corrosion. The temperature as well as charging voltage plays a considerable contribution towards the endurance of the battery. In general, the influence of temperature on the battery is always dealt with using the law in which elevated temperature produces a corrosion rate in higher. This is also applicable to the battery which is used for this research work. The battery should be kept at 25 °C in order to achieve the maximum lifetime of the battery at the time of standby service. The temperature of the battery and the environment temperature are obviously different. If the higher battery temperature is not in the hand to control for maintaining the battery life in a better way, meanwhile try to adjust the charging voltage as per the instruction manual given by the battery manufacturer is required to eliminate the serious decline towards service of the battery endurance. On the other hand, controlling the charging voltage is the pertinent requirement whether the battery temperature falls below 20 °C.



### 3.1 Thermal analysis using thermography

Infrared thermography is one of the widely used non-destructive evaluation technique to sense thickness variation and delamination. The principle of IRT is that electromagnetic radiation will be emitted by any material having a temperature above 0 K.<sup>19</sup> The IRT consists of IR camera which sense the emitted infrared energy by the object and at the same time shows the captured image (Figure 3) as a function of time. In the same way, any heat produced internally must transfer to the surface by means of either conduction or convection.<sup>20</sup> The thermal image (thermogram) taken from the IRT gives an exact relationship as a visual display among the intensity, emitted radiation spectral composition and the surface of the body.

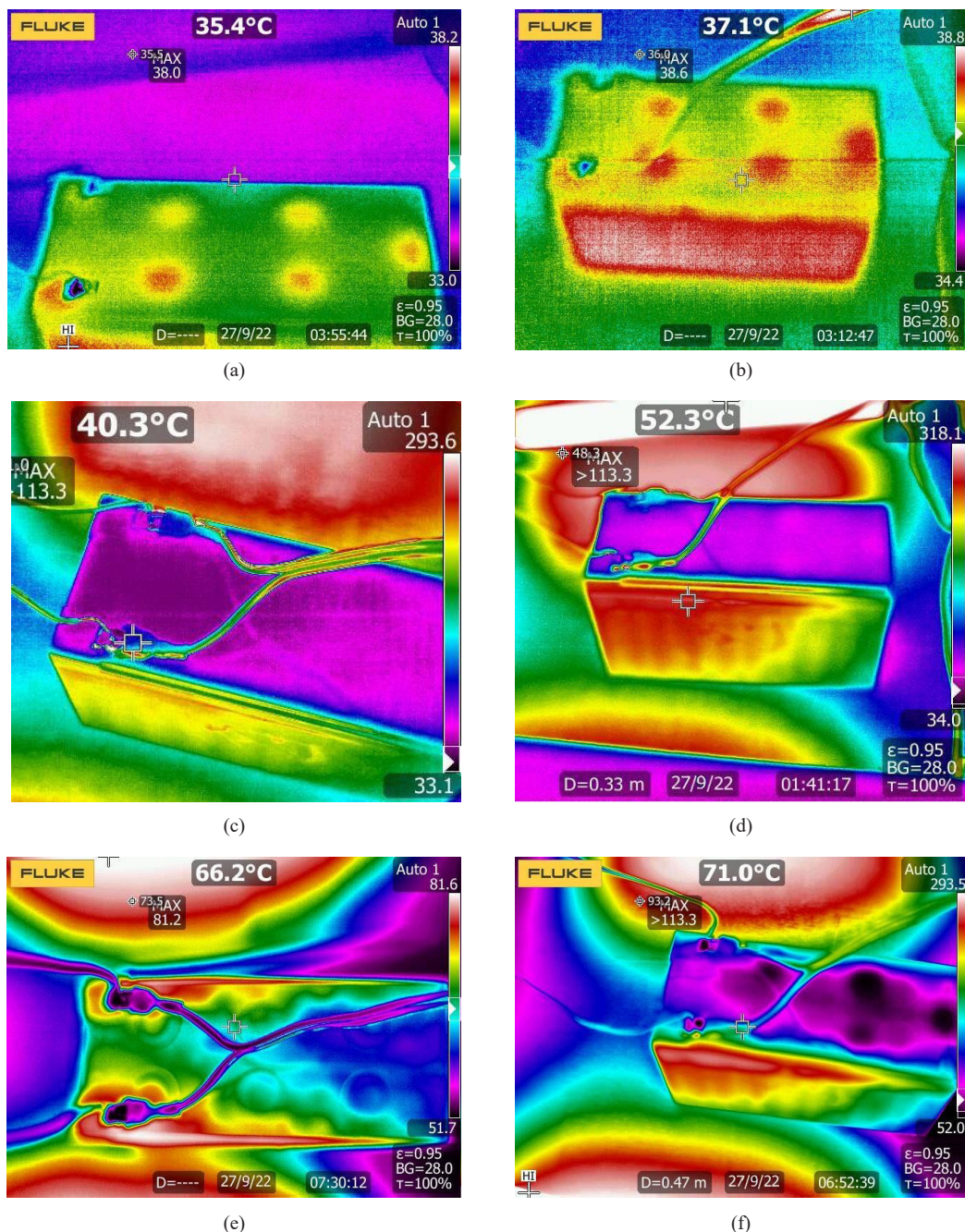


Figure 3. The thermography images on battery temperature variations at different timing

In the context of discharging a battery, the current distribution typically remains constant and stable. However, in experimental situations, there can be slight deviations from the steady state due to the delay in heat propagation. Figure 3 of the experiment demonstrates that the current density and distribution values vary from the actual values within specific time intervals, primarily due to transients. Specifically, the current density doubles for every 10% increase in water loss or every 10 degrees Celsius rise in temperature. Evaluating the battery's performance requires considering the dissipation of heat energy to the surrounding environment. Heat is dissipated through heat conduction in the battery's walls, which are solid mediums, as well as through convection with the surrounding environment. The voltage drop across the positive and negative plates is higher due to the lower resistance offered by these respective plates.

From Figure 3(a-f) shows the temperature variations of the battery at different timing. This Figure 3(a) shows the initial temperature of the battery connected to the load. Figure 3(d-f) show the high temperature exposure on the battery. At this period, the battery charging and discharging times are recorded very less. This will affect the battery's total capacity and also lead to an increase the resistance and improper chemical reactions. Due to all these points the battery is easily damaged and explosive. The improper chemical reaction causes corrosion on the plates and material deposition or sediment increases which leads to an increasing the internal resistance of the battery. These resistance variations block the electron moment in the plate which leads to temperature variations.

### 3.2 Differential scanning calorimetry analysis

From the Figure 4, the anode plate sample undergoes a gradual increase in thermal loading, while the corresponding glass transition temperature is measured. Initially, as the temperature rises, the material shows an exothermic behavior up to 150 °C. As the temperature continues to increase up to 375 °C, the material undergoes steady-state changes. However, at 400 °C, the material begins to exhibit an endothermic peak. A complex peak is observed at 424 °C with an onset value, a peak value of 432.1 °C, and a full degradation end value of 449.8 °C for the anode sample near the terminal point.

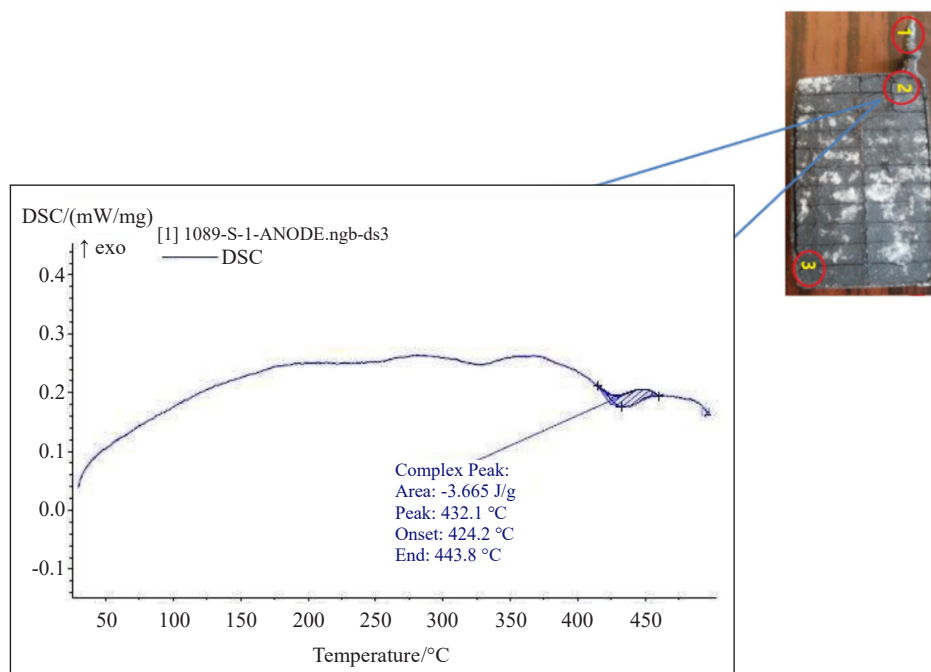
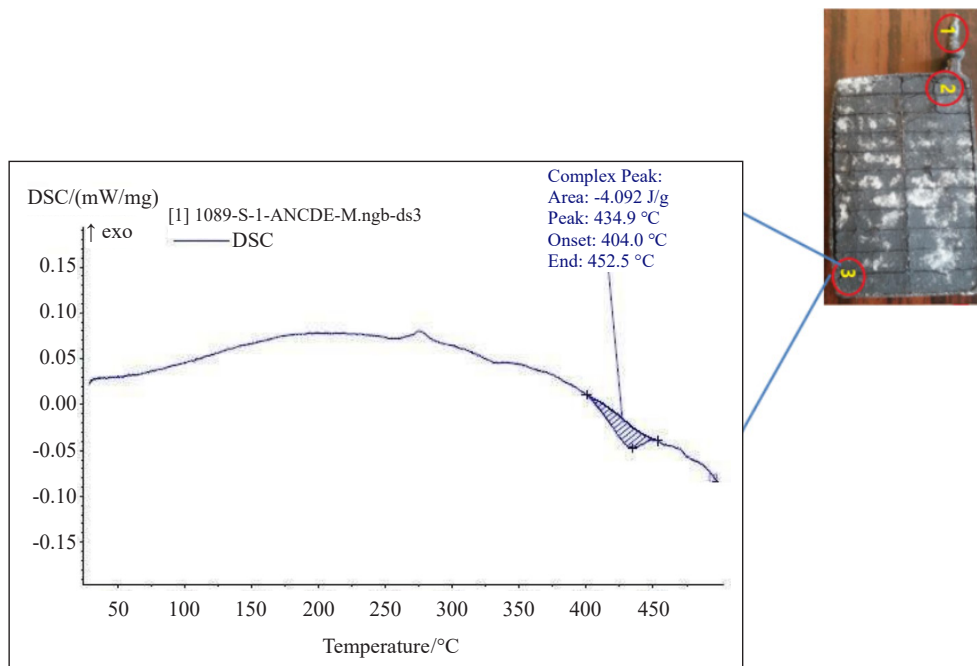
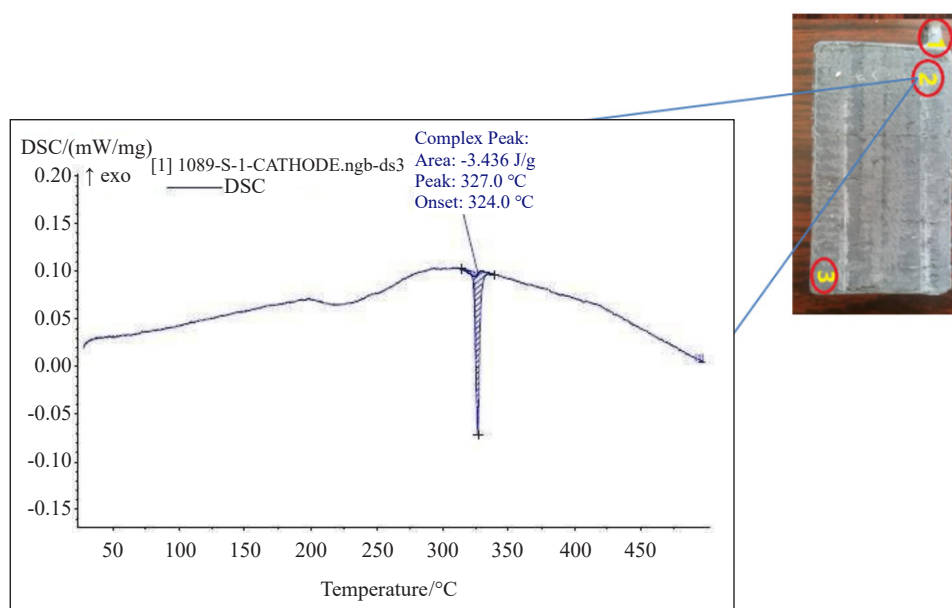


Figure 4. DSC analysis for anode plate at the point 2 position



**Figure 5.** DSC analysis for anode plate at the point 3 position

The findings illustrated in Figure 5 depict the outcomes obtained from the lower section of the anode plate. The recorded onset temperature is 404 °C, with a peak value of 434.5 °C and an end value of 452.5 °C. Based on these observations, it is evident that distinct thermal property fluctuations occur within a single plate, with an approximate temperature difference of 20 °C at the onset stage. These temperature variations can be attributed to changes in resistance, chemical reactions, plate corrosion, and material removal. If the temperature rises to its maximum level, it leads to an increased proportion of carbonates.



**Figure 6.** DSC analysis for Cathode plate at the point 2 position

The cathode material in Figure 6 displays a distinct, sharp peak indicating its crystalline behavior. Similar to the analysis of the anode, the cathode plate initially exhibits an exothermic nature but transitions into an endothermic behavior. The peak values are observed at 327 °C, with the onset temperature measured at 324 °C, indicating material melting at this temperature. Beyond the onset temperature, the material consistently exhibits an exothermic condition. Endothermic peaks at 250 °C and 260 °C suggest dehydration of hydrocarbonates, while the peak at 370 °C indicates decomposition.<sup>21</sup> It is essential for the positive plate to be sturdy enough to withstand mechanical stresses resulting from different molar volumes of the active material. In Figure 7, a sample taken from the bottom of the cathode plate shows a peak value of 326.3 °C and an onset value of 324.4 °C. These results provide clear evidence of structural transformation and changes in the plate's electrical properties due to charging/discharging cycles.

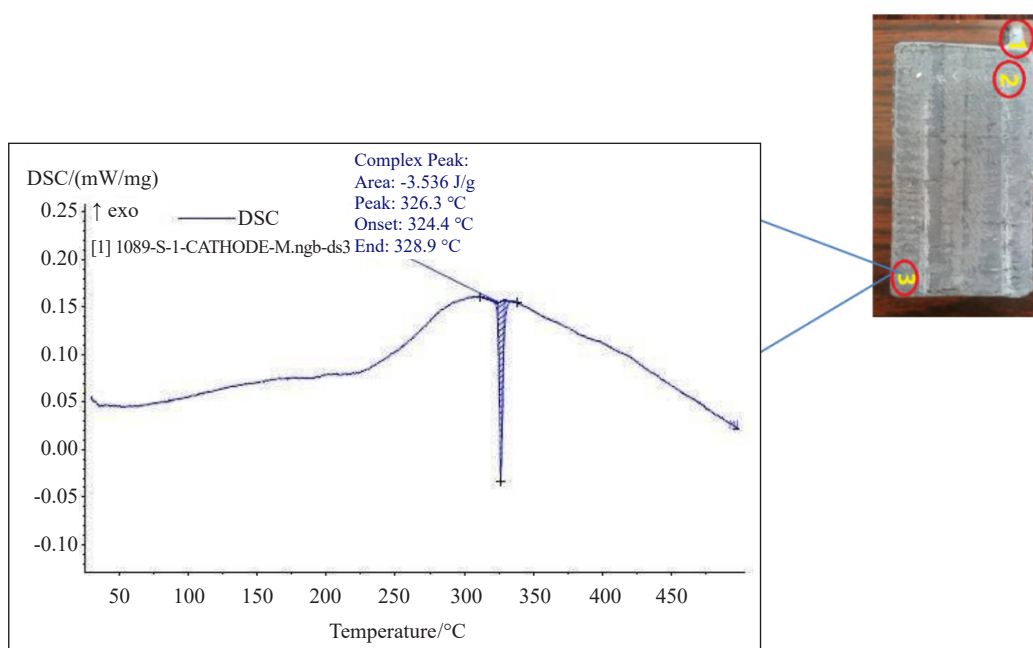


**Figure 7.** DSC analysis for Cathode plate at the point 3 position

### 3.3 Scanning electron microscope

The volume of the electrolyte is reduced due to gas leaving the vent when overcharging. As a result, few of the active materials pertaining to the battery lost contact with the electrodes. If the battery dried out completely or partially tends to raise the internal resistance of the battery in turn produces heat at the time of the charging process as well as accelerates water loss by means of evaporation.  $H_2SO_4$  is generated between the electrodes when charging. This higher concentrated acid with greater relative density has the tendency to deposit at the bottom of the lead acid battery. Due to privileged discharge at the upper parts of the battery as well as less ohmic resistance leads to acid stratification. Consequently, electrolyte concentration is lower momentarily in the upper part of the battery compared to the bottom of the battery. The concentration gradient occurs in the vertical direction directs towards poor usage of active mass as well as reduces the battery life during  $PbSO_4$  formation through an irreversible process, thus changing the morphology of the nanoparticles<sup>22</sup> Figure 8(a) shows the anode material SEM images (sample taken from the portion (2)). The images show the dry and large gap and discontinuity of the plate. This kind of material orientation leads to increasing the resistance and reducing the electron mobility. In Figure 8(b) images are taken from the anode plate bottom, in this only fewer voids and plate orientation are arranged properly. In comparison between Figure 8(a & b), the terminal was affected more due to heat and material removal from the plate increased due to chemical reactions.



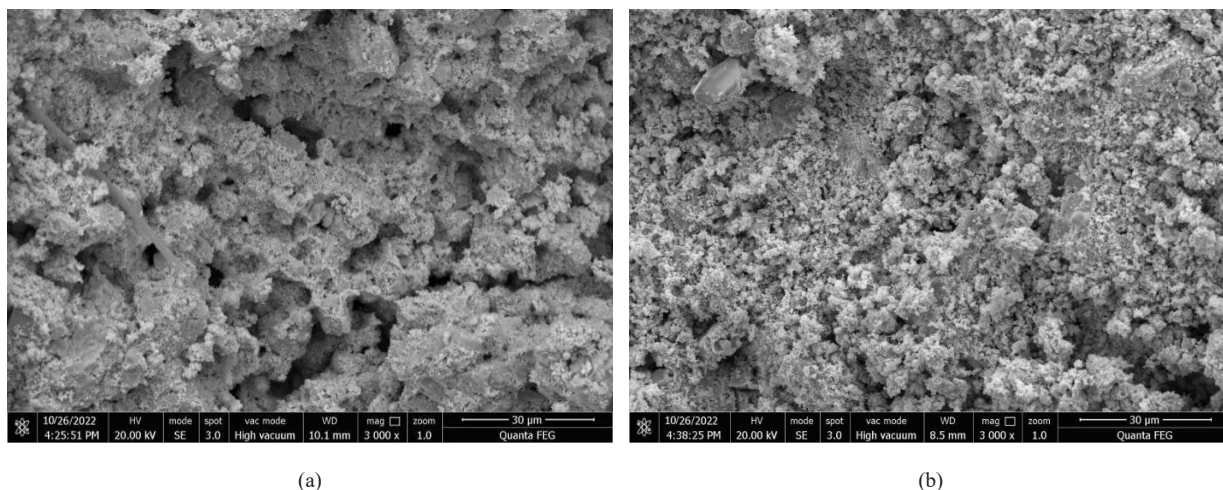


**Figure 8.** (a) Anode plate near the terminal, (b) Anode material sample from bottom of the plate

Figure 9(a) shows the cathode plate sample taken from near the terminal region, the material corrosion and pores are visible more compared with Figure 9(b). The reason behind this is the electrodes of the battery are not fully charged due to either physical variation at the electrode terminal to get the required potential or incorrect procedure of charging a battery. Thus, decelerate the battery capacity due to gradually increasing deposition of  $\text{PbSO}_4$  in the active area. The accumulation of  $\text{PbSO}_4$  over the electrode surface forms an insulation layer called sulphation. This sulphation occurs due to the standby of the battery in a discharge state very long time otherwise deficient charging state. During the sulphation process, small  $\text{PbSO}_4$  crystals produce large size crystals in turn increases the internal resistance of the battery meanwhile it is very difficult to convert back to active mass when its charging. In order to improve the stability of active mass, different nanomaterials are interfaced in the solid-solid interface section.<sup>23</sup>

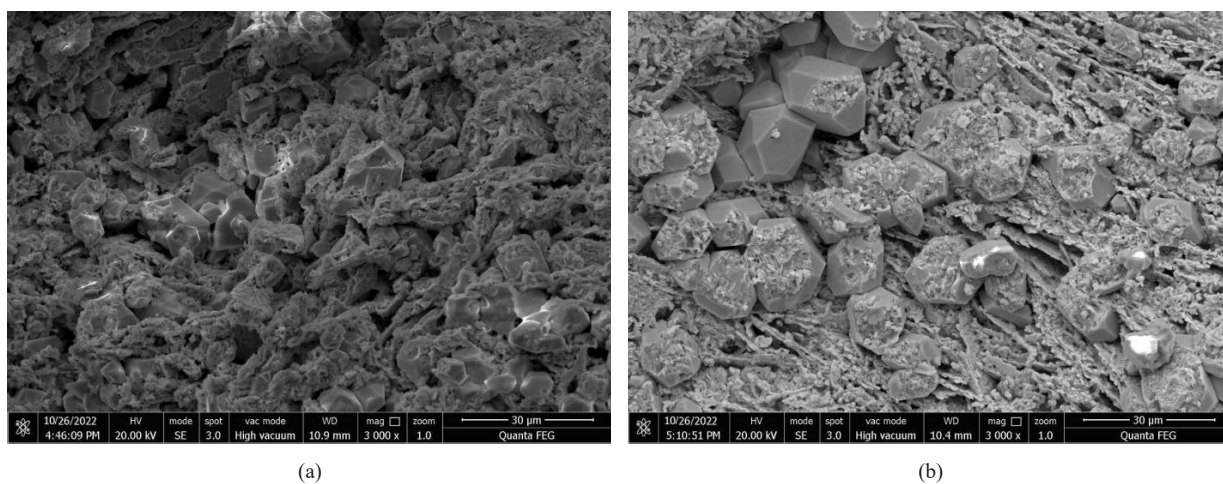


**Figure 9.** (a) Cathode plate near the terminal, (b) Cathode material sample from bottom of the plate

## 4. Conclusion

The thermal-influenced battery is dismantled like anode and cathode plates for thermal analysis. The test methods considered for this analysis DSC and SEM. Both methods are providing thermal influence over anode and cathode plates. DSC method provides the material temperature variations on plates under different conditions, results observed

that entire anode and cathode plates are exhibiting different thermal characteristics. All these changes happen because of temperature variations in the plate geometry. The SEM images are shown the anode and cathode plate conditions. In anode plate, the voids and material orientation are changed considerably. Further in the cathode plate also structural changes are observed. Maintaining a constant temperature will enhance the battery life. If the temperature increases the battery plate gets influenced and reduced the electron conductivity. Which leads the internal resistance variations followed by chemical changes in the battery.

## Conflict of interest

The authors declare no competing financial interest.

## References

- [1] Chatzivasileiadi, A.; Ampatzis, E.; Knight, I. Characteristics of electrical energy storage technologies and their applications in buildings. *Renewable and Sustainable Energy Reviews*. **2013**, *25*, 814-830.
- [2] Dell, R. M. Batteries: fifty years of materials development. *Solid State Ionics*. **2000**, *134*, 139-158.
- [3] Ouyang, D.; Chen, M.; Wei, R.; Wang, Z.; Wang, J. A study on the fire behaviors of 18650 battery and batteries pack under discharge. *Journal of Thermal Analysis and Calorimetry*. **2019**, *136*, 1915-1926.
- [4] Song, X.; Hu, S.; Chen, D.; Zhu, B. Estimation of waste battery generation and analysis of the waste battery recycling system in China. *Journal of Industrial Ecology*. **2017**, *21*, 57-69.
- [5] Daniel, C.; Besenhard, J. O. *Handbook of Battery Materials*. John Wiley & Sons, 2012.
- [6] Pavlov, D. *Lead-Acid Batteries: Science and Technology*. Elsevier, 2011.
- [7] Yang, J.; Hu, C.; Wang, H.; Yang, K.; Liu, J. B.; Yan, H. Review on the research of failure modes and mechanism for lead-acid batteries. *International Journal of Energy Research*. **2017**, *41*, 336-352.
- [8] Ryś, P. A.; Lipkowski, J.; Siekierski, M.; Biczal, P. The effect of various buffer battery maintenance regimes on the state of health of VRLA batteries. *Journal of Power Technologies*. **2019**, *98*, 365-376.
- [9] Tomantschger, K.; Valeriotte, E. M.; Sklarchuk, J.; Chang, T. G.; Dewar, M. J.; Ferrone, V.; Jochim, D. M. Laboratory and field evaluations of Optima VRLA batteries utilizing rapid charging. In *Thirteenth Annual Battery Conference on Applications and Advances*. Proceedings of the Conference, IEEE, 1998; pp 173-178.
- [10] Tong, P.; Zhao, R.; Zhang, R.; Yi, F.; Shi, G.; Li, A.; Chen, H. Characterization of lead (II)-containing activated carbon and its excellent performance of extending lead-acid battery life for high-rate partial-state-of-charge operation. *Journal of Power Sources*. **2015**, *286*, 91-102.
- [11] Culpin, B. Thermal runaway in valve-regulated lead-acid cells and the effect of separator structure. *Journal of Power Sources*. **2004**, *133*, 79-86.
- [12] Rand, D. A. J.; Holden, L. S.; May, G. J.; Newnham, R. H.; Peters, K. Valve-regulated lead/acid batteries. *Journal of Power Sources*. **1996**, *59*, 191-197.
- [13] Chang, Y.; Mao, X.; Zhao, Y.; Feng, S.; Chen, H.; Finlow, D. Lead-acid battery use in the development of renewable energy systems in China. *Journal of Power Sources*. **2009**, *191*, 176-183.
- [14] Hu, J.; Guo, Y.; Zhou, X. Thermal runaway of valve-regulated lead-acid batteries. *Journal of Applied Electrochemistry*. **2006**, *36*, 1083-1089.
- [15] Mohanty, D.; Hockaday, E.; Li, J.; Hensley, D. K.; Daniel, C.; Wood III, D. L. Effect of electrode manufacturing defects on electrochemical performance of lithium-ion batteries: Cognizance of the battery failure sources. *Journal of Power Sources*. **2016**, *312*, 70-79.
- [16] Pesaran, A. A.; Vlahinos, A.; Burch, S. D. *Thermal Performance of EV and HEV Battery Modules and Packs*. National Renewable Energy Laboratory, 1997.
- [17] Nakamura, K.; Shiomi, M.; Takahashi, K.; Tsubota, M. Failure modes of valve-regulated lead/acid batteries. *Journal of Power Sources*. **1996**, *59*, 153-157.
- [18] Yamaguchi, Y.; Shiota, M.; Nakayama, Y.; Hirai, N.; Hara, S. Combined in situ EC-AFM and CV measurement study on lead electrode for lead-acid batteries. *Journal of Power Sources*. **2001**, *93*, 104-111.
- [19] Streza, M.; Nuț, C.; Tudoran, C.; Bunea, V.; Calborean, A.; Morari, C. Distribution of current in the electrodes of lead-acid batteries: a thermographic analysis approach. *Journal of Physics D: Applied Physics*. **2016**, *49*, 055503.

- [20] Sivaraj, P.; Abhilash, K. P.; Selvin, P. C. A critical review on electrochemical properties and significance of orthosilicate-based cathode materials for rechargeable Li/Na/Mg batteries and hybrid supercapacitors. *ChemistrySelect*. **2021**, *6*, 12036-12073.
- [21] Yong, B.; Tian, Y.; Yang, B.; Xu, B.-Q.; Liu, D.-C.; Wang, F.; Xiong, N.; Zhang, W. Vacuum decomposition thermodynamics and experiments of recycled lead carbonate from waste lead acid battery. *Thermal Science*. **2021**, *25*.
- [22] Sivaraj, P.; Abhilash, K. P.; Nalini, B.; Balraju, P.; Yadav, S. K.; Jayapandi, S.; Christopher Selvin, P. Structure, dielectric, and temperature-dependent conductivity studies of the  $\text{Li}_2\text{FeSiO}_4/\text{C}$  nano cathode material for lithium-ion batteries. *Ionics*. **2019**, *25*, 2041-2056.
- [23] Parameswaran, A. K.; Azadmanjiri, J.; Palaniyandy, N.; Pal, B.; Palaniswami, S.; Dekanovsky, L.; Wu, B.; Sofer, Z. Recent progress of nanotechnology in the research framework of all-solid-state batteries. *Nano Energy*. **2022**, 107994.